CO adsorption on the reduced $RuO_2(110)$ surface: Energetics and structure

Ari P. Seitsonen,* Y. D. Kim, M. Knapp, S. Wendt, and H. Over†
Abteilung Physikalische Chemie, Fritz-Haber-Institut der Max-Planck-Gesellschaft, Faradayweg 4-6, D-14195 Berlin, Germany
(Received 5 September 2001; published 27 December 2001)

The adsorption sites of CO on the reduced $RuO_2(110)$ surface were determined by employing the techniques of density-functional theory calculations and quantitative low-energy electron diffraction. On the mildly reduced $RuO_2(110)$ surface, where the bridging oxygens are removed, twofold (2f) undercoordinated Ru atoms [2f- coordinatively unsaturated site (cus) Ru] are exposed. On this surface, the CO molecules initially adsorb above these 2f-cus Ru atoms in symmetric bridge positions. The CO coordinated 2f-cus Ru atoms are drawn towards the CO molecule by 0.2 Å. With increasing CO coverage, the CO adsorption site changes from the symmetric to the asymmetric bridge position. When all 2f-cus Ru atoms have been capped by bridging CO molecules, the 1f-cus Ru atoms are also progressively occupied by on-top CO. For comparison, on the stoichiometric $RuO_2(110)$ surface, CO molecules adsorb exclusively on top of the onefold coordinatively unsaturated Ru atoms (1f-cus Ru) at temperatures below 200 K. The energetics of the CO adsorption on the reduced $RuO_2(110)$ surface compares favorably with the corresponding thermal-desorption spectrum.

DOI: 10.1103/PhysRevB.65.035413 PACS number(s): 68.43.Fg, 61.14.Hg, 31.15.Ar, 81.65.Mq

I. INTRODUCTION

Ruthenium dioxide has shown to be extraordinarily active in oxidizing CO molecules,[1–4] an effect that has been traced to the presence of undercoordinated atoms at the RuO_2 surface.[1,2] In bulk RuO_2, which crystallizes in the rutile structure like TiO_2, the Ru atoms are coordinated to six O atoms in an octahedral configuration, while the O atoms are (planar-) coordinated to three Ru atoms. The RuO_2 surface with the lowest surface energy is the stoichiometric $RuO_2(110)$, which stabilizes two kinds of undercoordinated atoms [cf. Fig. 1(a)]: First, the so-called onefold coordinatively unsaturated site (1f-cus) Ru atoms, which are attached to five instead of six O atoms, and second, the bridging O atoms, which are coordinated to two rather than to three Ru atoms.[5]

The microscopic steps of the CO oxidation reaction at a $RuO_2(110)$ film on Ru(0001) were unraveled by a combined endeavor, applying the experimental techniques of low-energy electron diffraction (LEED) and scanning tunneling microscopy in combination with state-of-the-art density-functional theory (DFT) calculations.[1] The catalytically active centers on $RuO_2(110)$ have been identified with the undercoordinated Ru and oxygen atoms at the surface. CO molecules adsorb first in terminal position above the 1f-cus Ru atoms from where they recombine with the (undercoordinated) bridging oxygen atoms.[1,6,7]

Under mildly reducing conditions, the stoichiometric $RuO_2(110)$ is reduced via the removal of bridging oxygen atoms which are partially replaced by the reducing agent such as CO molecules.[7] Such a mildly reduced $RuO_2(110)$ surface [in the following, referred to as r-$RuO_2(110)$] exposes two kinds of undercoordinated Ru atoms, i.e., the twofold undercoordinated 2f-cus Ru and the 1f-cus Ru atoms, exhibiting two and one ''dangling bonds,'' respectively [cf. Fig. 1(b)]. Intuitively one expects the CO molecules to adsorb preferentially above the 2f-cus Ru atoms, since those sites offer two dangling bonds with which the CO molecule can bond. This view will be shown to be too simple for predicting the actual adsorption geometries.

In the present paper we explore the energetics and the local adsorption geometries of CO on the r-$RuO_2(110)$ surface as a function of the CO coverage. The results are compared with those for CO adsorbed on the stoichiometric $RuO_2(110)$ surface, which is referred to as s-$RuO_2(110)$.

II. TECHNICAL DETAILS OF THE EXPERIMENTS AND THE CALCULATIONS

The measurements were conducted in a UHV chamber[8] which is equipped with four-grid back-view LEED optics,

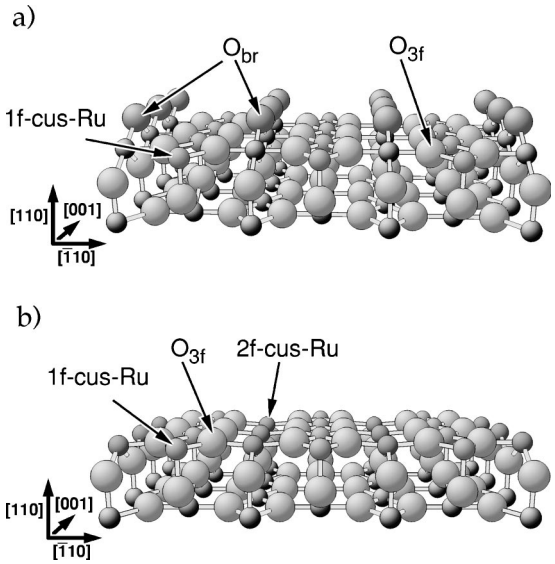

FIG. 1. Stick and ball model of the pristine (a) and completely reduced (b) $RuO_2(110)$ surface. Large balls represent oxygen, and small balls represent ruthenium atoms of $RuO_2(110)$. The pristine surface exposes bridging oxygen O_{br} and Ru atoms (1f-cus Ru). On the reduced $RuO_2(110)$ surface, the undercoordinated O atoms are removed, thus exposing two kinds of undercoordinated Ru atoms: 1f-cus Ru and 2f-cus Ru.

Auger electron spectroscopy, thermal-desorption spectroscopy, and facilities to clean and prepare the Ru(0001) surface. The sample temperature could be varied from 100 K (by cooling with liquid N_2) to 1530 K (by direct resistive heating). The LEED intensities as a function of the incident electron energy were collected at normal incidence of the primary beam and a sample temperature of 100 K. A computer-controlled highly sensitive charge-coupled device camera was used to record spot intensities from the LEED fluorescence screen. LEED $I(V)$ curves were computed by using the program code of Moritz[9] and compared with the experimental LEED $I(V)$ curves by applying a least-squares optimization algorithm,[10] based on Pendry's r factor R_P.[11] A Pendry's r factor of 0.0 means perfect agreement between two LEED data sets, while a value of 1.0 expresses uncorrelated data sets.

The $RuO_2(110)$ phase was produced by exposing a well-prepared single-crystal Ru(0001) surface to high doses of oxygen at an elevated sample temperature of 700 K. Typical oxygen exposures for the preparation were several 10^6 L. After the background pressure in the UHV chamber had reached a value below 10^{-9} mbar, the sample was briefly flashed to 600 K in order to remove contamination by residual gas (in particular, oxygen) adsorption. For the measurements the sample was cooled to 100 K. The so-prepared oxygen-rich phase on Ru(0001) exposes primarily $RuO_2(110)$ areas in coexistence with small areas of (1×1)-O. In order to produce the reduced $RuO_2(110)$ surface, the surface was exposed several times (typically, five to ten times) to 0.25 L CO at 170 K and annealed to 550 K while monitoring the CO_2 signal with a quadrupole mass spectrometer. As soon as the CO_2 signal has vanished, the resulting surface is considered as the reduced $RuO_2(110)$. This simple recipe is based on recent high-resolution electron-energy-loss spectroscopy (HREELS) measurements,[7] which indicated that exposing the $RuO_2(110)$ to CO at room temperature depletes the amount of bridging oxygen gradually until at a cumulative exposure of about 1 L CO all bridging O atoms are consumed, i.e., the stoichiometric $RuO_2(110)$ turns into a reduced $RuO_2(110)$ surface where part of the 2f-cus Ru atoms are capped by bridging CO molecules. At sample temperatures below 500 K the r-$RuO_2(110)$ surface is no longer able to convert CO to CO_2 without dosing additional oxygen.

For the DFT calculations we employed the generalized gradient approximation of Perdew, Burke, and Ernzerhof[12] for the exchange-correlation functional. We used *ab initio* pseudopotentials, created with the scheme of Troullier and Martins,[13] in the fully separable form. The electronic wave functions were expanded in a plane-wave basis set with an energy cutoff of 60 Ry. The r-$RuO_2(110)$ and s-$RuO_2(110)$ surfaces were modeled in the supercell approach by five double layers in a symmetric slab geometry. CO molecules were put on both sides of the RuO_2 slab (either reduced or stoichiometric) so that the inversion symmetry was preserved. A vacuum region of about 16 Å was employed to decouple the surfaces of consecutive slabs in the supercell approach. Calculations were performed using (1×1) and (2×1) surface unit cells to study the coverage dependence. The integral over the Brillouin zone was performed using a special k-point set,[14] with eight and four k points in the irreducible part of the (1×1) and the (2×1) Brillouin zones, respectively. To accelerate the electronic relaxation, Fermi broadening of the occupation numbers was used with a width of 0.1 eV, and the energies were extrapolated to zero temperature. All the atoms were allowed to relax.

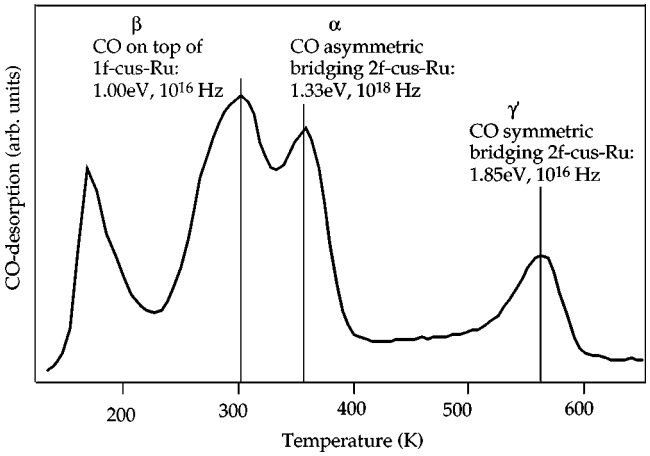

FIG. 2. CO thermal-desorption spectrum from a completely reduced $RuO_2(110)$ surface, i.e., all bridging O atoms have been removed. The differential heat of adsorption is determined by DFT calculations, while the frequency factors are estimated by applying the Readhead formula (Ref. 16).

III. RESULTS AND DISCUSSION

A. Energetics

In Fig. 2 we show the CO desorption spectrum from the reduced $RuO_2(110)$ surface. Three desorption states can clearly be discriminated: the low-temperature states α and β and the high-temperature desorption state γ'. The CO desorption behavior is much simpler for CO on r-$RuO_2(110)$ than on the s-$RuO_2(110)$ surface, since almost all CO molecules on the reduced surface leave the surface as CO molecules and do not form CO_2 in contrast to the stoichiometric $RuO_2(110)$ surface. From the present DFT calculations the various desorption states can be attributed to particular CO adsorption sites. These assignments are also supported by full-dynamical LEED analyses.

In Table I we summarize the DFT calculations for the various CO adsorption sites and CO coverages on r-$RuO_2(110)$. The coverage-dependent occupation of CO adsorption sites is summarized in Fig. 3. For low coverages (on the average only every second 2f-cus Ru atom is occupied) the symmetric bridge position above 2f-cus Ru atoms is the preferred adsorption site with 1.85 eV, followed by the on-top position above 1f-cus Ru atoms (1.61 eV). The adsorption energy and the adsorption geometry depend critically on the CO coverage. By capping all dangling bonds of the 2f-cus Ru atoms, the preference changes from the symmetric bridge position to the asymmetric bridge position above the 2f-cus Ru atoms (averaged adsorption energy, 1.59 eV). The adsorption energy at the asymmetric bridge position is degenerate with the configuration where 0.5 ML CO is

TABLE I. Calculated (averaged) DFT binding energies $E(\theta)$ for the system CO on reduced and stoichiometric $RuO_2(110)$ for various adsorption sites, and the binding energies of the bridging O atoms. CO_{s-br}: CO molecules symmetrically bridging 2f-cus Ru atoms. CO_{a-br}: CO molecules asymmetrically bridging 2f-cus Ru atoms. CO_{ot-1f}: CO molecules adsorb on top of the 1f-cus Ru atoms. CO_{ot-2f}: CO molecules adsorb on top of the 2f-cus Ru atoms. O_{br}: Bridging oxygen atom.

System	$E(\theta)$ (eV)
r-$RuO_2(110)$-(1×1)	
CO_{ot-2f}	1.04
CO_{s-br}	1.30
CO_{a-br}	1.59
CO_{ot-1f}	1.46
r-$RuO_2(110)$-(2×1)	
CO_{ot-2f}	0.95
CO_{s-br}	1.85
CO_{ot-1f}	1.61
r-$RuO_2(110)$-(2×1)	
$1O_{br}+CO_{s-br}$	1.51
$1O_{br}+CO_{a-br}$	1.73
$1O_{br}$	1.60
$2O_{br}$	1.60

TABLE II. Calculated (averaged) DFT binding energies $E(\theta)$ for the system CO on reduced and stoichiometric $RuO_2(110)$ [r-$RuO_2(110)$ and s-$RuO_2(110)$, respectively]. E_{diff} is the differential heat of adsorption as defined in the text. The annotation is the same as in Table I.

System	θ_{CO}	$E_{CO}(\theta)$ (eV)	E_{diff} (eV)
r-$RuO_2(110)$-(2×1)			
			$1/2\rightarrow0$:1.85
$1CO_{s-br}$	1/2	1.85	
$1CO_{ot-1f}$	1/2	1.61	
			$1\rightarrow1/2$:1.33
$2CO_{a-br}$	1	1.59	
$1CO_{s-br}+1CO_{ot-1f}$	1	1.62	
$2CO_{ot-1f}$	1	1.46	
			$3/2\rightarrow1$:1.32
$2CO_{a-br}+1CO_{ot-1f}$	3/2	1.50	
$1CO_{s-br}+2CO_{ot-1f}$	3/2	1.37	
			$2\rightarrow3/2$:0.74
$2CO_{a-br}+2CO_{ot-1f}$	2	1.31	
s-$RuO_2(110)$-(2×1)			
			$1/2\rightarrow0$:1.30
$1CO_{ot-1f}$	1/2	1.30	
			$1\rightarrow1/2$:1.10
$2CO_{ot-1f}$	1	1.20	

located in the symmetric bridge position above the 2f-cus Ru atoms and 0.5 ML CO is situated in the on-top configuration above the 1f-cus Ru atoms. Although the binding energies are similar, the frequency factors, and accordingly the entropy terms, of these configurations should be quite different since the diffusion barrier along the 2f-cus Ru atoms and along the 1f-cus Ru atoms are 0.9 eV and 1.1 eV, respectively. Therefore it is not clear from the DFT calculations which configuration is the stable one at finite temperature, in particular at temperatures close to desorption. If complete rows of cus Ru atoms (either 2f-cus Ru or 1f-cus Ru) are occupied, the on-top position at the 1f-cus Ru atoms is even more favorable than the symmetric bridge position between 2f-cus Ru atoms. We may add that at the beginning of our study DFT and LEED calculations arrived at different conclusions about the adsorption site. While LEED favored the symmetric bridge position above the 2f-cus Ru atoms, DFT favored the CO adsorption on top of the 1f-cus Ru position. This discrepancy was resolved by the discovery of the asymmetric bridge position. At even higher CO coverages also the 1f-cus Ru atoms are occupied by on-top CO. In addition, an interesting result is that the adsorption energy of CO in a bridging O vacancy is as high as 1.73 eV. This means that whenever a bridging O vacancy has been formed, CO will move from the on-top site above the 1f-cus Ru atom toward the vacancy due to thermodynamics if the kinetic limitation can be overcome.

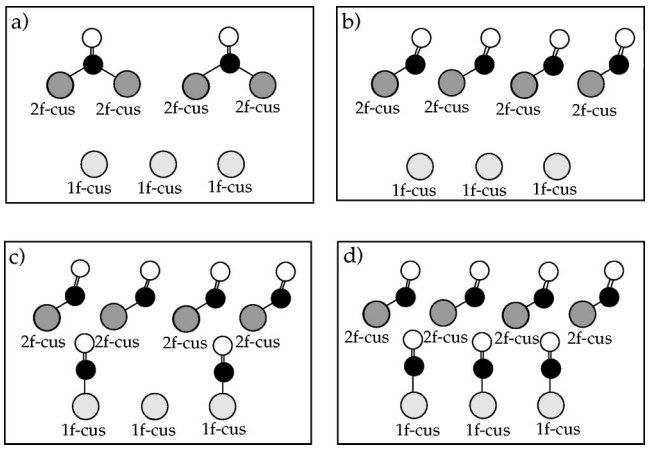

FIG. 3. Schematic diagram of the adsorption sites of CO on the reduced $RuO_2(110)$ surface as a function of the CO coverage. These sites were determined by the DFT calculations.

The CO bonding is considered to be mainly determined by the first coordination shell of the CO molecules, i.e., the adsorption site. Our DFT calculations reveal, however, that the binding energy of CO on top of the 1f-cus Ru atoms is rather sensitive to the presence of bridging oxygen atoms, which are located in the third coordination shell. While the binding energy is only 1.20 eV for the case of the s-$RuO_2(110)$ surface, this value increases to 1.46 eV when the bridging O atoms have been removed. Obviously the various surface Ru atoms interact quite strongly via the attached in-plane oxygen atoms (O_{3f} in Fig. 1).

In Table II we summarize the (averaged) CO binding energy $E(\theta)$ together with the differential ''heat of adsorption'' E_{diff} as a function of the CO coverage. E_{diff} is defined as

TABLE III. Pendry's r factor values between experimental LEED data sets for various preparation conditions. Bold numbers indicate ''identical'' LEED data sets; italic numbers, indifferent. A: $3\times$(5 L CO at 285 K, heating to 400 K), B: A+5 L CO at 120 K, C: B+heating to 210 K, D: C+heating to 285 K, E: D+heating to 360 K, and F: E+heating to 665 K annealing for 5 minutes. r factors between various surface preparations: B vs C: 0.13, C vs D: 0.20, D vs E: 0.15, and E vs F: 0.34.

System	A	B	C	D	E	F
Stoichiometric $RuO_2(110)$ (1)	0.31	0.60	0.53	0.30	0.30	**0.12**
Stoichiometric $RuO_2(110)$ (2)	0.31	0.65	0.59	0.34	0.33	**0.10**
s-$RuO_2(110)$: 10 L CO at 300 K	0.19	0.62	0.54	0.14	0.14	0.42
s-$RuO_2(110)$: 10 L CO at 300 K + 5 L at 50 K	0.57	**0.10**	0.17	0.42	0.60	0.66
A	**0**	0.58	0.32	0.15	**0.05**	0.28

$$E_{\mathrm{diff}}(\theta_1 \rightarrow \theta_2) = \frac{\theta_2 E(\theta_2) - \theta_1 E(\theta_1)}{\theta_2 - \theta_1}, \qquad (1)$$

i.e., E_{diff} is the discrete derivative of $\theta \cdot E(\theta)$, the integral heat of adsorption. For first-order desorption the differential heat of adsorption approximates the activation energy for desorption and is therefore the chemically relevant quantity to compare with experimental thermal-desorption spectra.[15]

For a thorough discussion of thermal-desorption spectra also the (attempt) frequency factor is an important quantity which is directly related to the entropy gain in the course of desorption. To estimate the frequency factors we used the Readhead formula.[16] According to the transition state theory[17] the entropy gain during desorption is directly related to the attempt frequency of the CO molecule to overcome the activation barrier for desorption, i.e., how many times per second the CO molecules run against the activation barrier for desorption. A commonly used value for the frequency factor is 10^{13} Hz, which assumes that the adlayer is completely mobile on the surface. However, for localized adsorption the entropy between the initial state and the desorption state of CO (identical to the transition state for first-order desorption) is different by several orders of magnitude.[18] Strong localization of the CO molecule on s-$RuO_2(110)$ is suggested by the corresponding diffusion barriers of CO on the surface which are about 1 eV.

Let us now return to the discussion of the desorption states α, β, and γ' in Fig. 2. The low-temperature state at 180 K has not been identified so far. From the DFT calculations the desorption states at 300 K correspond to CO in the terminal position above 1f-cus Ru, but the state at 365 K is ascribed to CO molecules asymmetrically bridging the 2f-cus Ru atoms. The high-temperature desorption state at 560 K (γ' state) is related to symmetrically bridging CO molecules adsorbed above the 2f-cus Ru atoms in a diluted phase. Combining the calculated values for different heat of adsorption with the Readhead formula, we estimated the corresponding frequency factors which are in the range of 10^{16} to 10^{18} Hz. These high values corroborate the strong localization of the CO layers on the r-$RuO_2(110)$ surface consistent with the estimated diffusion barriers, i.e., 0.9 eV along the 1f-cus Ru atoms and 1.1 eV along the 2f-cus Ru atoms.

The found CO adsorption sites based on our DFT calculations are consistent with recent HREELS data of CO adsorbed on the reduced $RuO_2(110)$ surface.[19] Annealing at 300 K a previously (with CO) saturated r-$RuO_2(110)$ surface reveals two vibrational losses at 235 meV and 245 meV, which were assigned to CO molecules attached to 2f-cus Ru rather than to 1f-cus Ru atoms. Specific bonding geometries for these CO species were not offered by the authors since it is well documented that HREELS is not reliable in deducing the adsorption site of CO; in particular this technique failed several times for the discrimination between bridge and on-top positions.[20] With the DFT calculations we are now able to assign these vibrational losses to specific adsorption geometries. The vibrational loss at 235 meV is related to CO in the symmetric bridging position above 2f-cus Ru atoms, while the loss at 245 meV is ascribed to CO sitting in the asymmetric bridge position above the 2f-cus Ru atoms [cf. Figs. 3(a) and 3(b)]. The lower vibrational energy of the symmetric bridging CO is also consistent with a higher degree of back donation (see below) than for the case of the asymmetric bridge CO position. For comparison, the DFT-calculated vibrational frequencies are 238 meV for the symmetrical bridging CO above the 2f-cus Ru atom, 247 meV for the asymmetrical bridging CO above the 2f-cus Ru atoms, and 258 meV for on-top CO above the 1f-cus Ru atoms. These values are in excellent agreement with experiment.

B. Adsorption geometries

With LEED (either quantitative or in the fingerprinting mode[21]), we studied the surface structures of various CO phases on the reduced $RuO_2(110)$ surface. We saturated the reduced $RuO_2(110)$ surface with CO and then heated the sample to predetermined temperatures in order to depopulate specific desorption states (cf. Fig. 2). In Table III we compare these experimental LEED data sets for various CO overlayers with those of the clean $RuO_2(110)$ surface and differently prepared CO overlayers. More specifically, we started with a reduced $RuO_2(110)$ surface which was prepared by three cycles of 5 L CO exposure at 170 K and flashing to 400 K; this preparation method is referred to as surface A. Surface B is produced by exposing an additional 5 L CO at 120 K to surface A. Subsequently, this surface was flashed to 210 K (surface C), 285 K (surface D), 360 K (surface E), and finally to 665 K for 5 minutes (surface F). For the surfaces A–F complete experimental LEED data sets were taken at 100 K. The comparison among the experimental data sets is

TABLE IV. Optimum Pendry's *r* factor achieved with various model structures for the $RuO_2(110)$ surface that was exposed to 10 L CO at 300 K. The best *r* factors are given in bold. CO_{s-br}: CO molecules symmetrically bridging 2f-cus Ru atoms. CO_{a-br}: CO molecules asymmetrically bridging 2f-cus Ru atoms. CO_{br-1f}: CO molecules symmetrically bridging 1f-cus Ru atoms. CO_{ot-1f}: CO molecules adsorb on-top of the 1f-cus Ru atoms. CO_{ot-2f}: CO molecules adsorb on-top of the 2f-cus Ru atoms. CO_{br-O}: bridging CO molecules above bridging O atoms. CO_{ot-O}: CO molecules on-top above bridging O atoms.

Model structure	Optimum *r* factor
r-$RuO_2(110)$	
CO_{ot-1f}	0.67
CO_{br-1f}	0.61
Bare surface	0.54
CO_{ot-2f}	0.72
CO_{br-2f} + CO_{br-1f}	0.52
CO_{ot-1f} + CO_{br-2f}	0.61
CO_{ot-1f} + 0.5 CO_{br-2f}	0.40
CO_{ot-2f} + CO_{br-1f}	0.67
CO_{ot-2f} + CO_{ot-1f}	0.69
CO_{ot-2f}	**0.29**
CO_{a-br}	**0.27**
s-$RuO_2(110)$	
Bare surface	0.46
CO_{br-1f}	0.53
CO_{ot-1f}	0.52
O_{br} + CO_{br-O}	0.59
O_{br} + CO_{ot-O}	0.86

quantified by using Pendry's *r* factor. If two experimental LEED data sets are very similar (i.e., Pendry's *r* factor is low, say, below 0.10–0.15) then also the local adsorption geometries of the ordered part of the surface are very similar; note that the reproducibility of experimental LEED data is quantified by 0.08. This kind of approach is termed the LEED fingerprinting technique, whose utility and broad applicability have been demonstrated by a manifold of instructing examples.[21]

In order to produce the reduced $RuO_2(110)$ surface one can also expose the stoichiometric $RuO_2(110)$ surface to 10 L CO at 300 K. According to the recent HREELS study[7] this should lead to a surface where no bridging oxygen is left on the surface and where part of the 2f-cus Ru atoms are saturated by CO molecules. A LEED analysis of this phase revealed that indeed the bridging O atoms are replaced by CO molecules residing above the 2f-cus Ru atoms in an asymmetric bridge configuration, while no CO is sitting above the 1f-cus Ru atoms. This surface was then exposed to 5 L CO at 50 K in order to occupy also the low-energy adsorption sites. Again a complete LEED analysis of this phase showed that in addition to the asymmetric bridge positions, CO molecules occupy the 1f-cus Ru atoms in the on-top position.

The quantitative comparison among the experimental LEED data sets suggests the following conclusions (cf. Table IV): Surface A and the surface with CO in the asymmetric

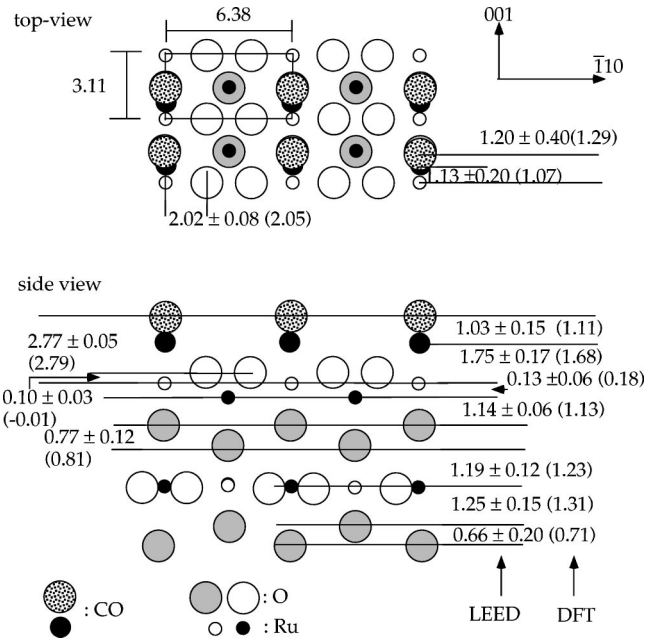

FIG. 4. The optimum surface geometry of the CO on the reduced $RuO_2(110)$ surface, when the stoichiometric $RuO_2(110)$ surface is exposed to 10 L CO at room temperature. The structure was determined by LEED and DFT calculations (parameter values are in parentheses). CO sits in an asymmetric bridge position above 2f-cus Ru atoms. All values are in argstrom. The corresponding layer spacings in bulk RuO_2 are 1.27 Å and 0.635 Å.

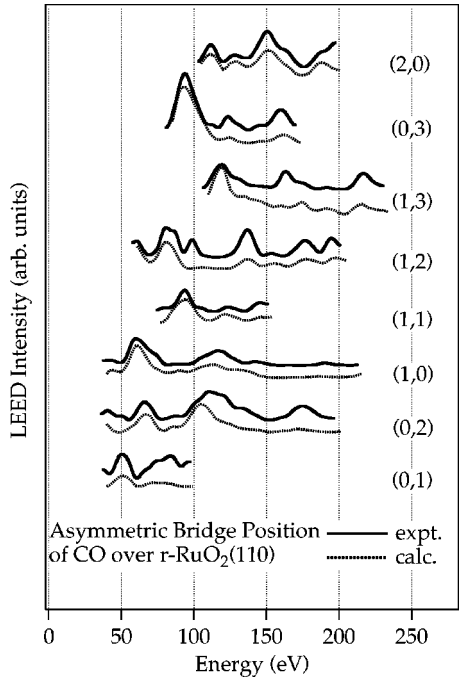

FIG. 5. Comparison of experimental LEED I(V) data and simulated LEED I(V) curves for the CO-$RuO_2(110)$ with CO sitting in the asymmetric bridge position above 2f-cus Ru atoms. The optimum R_P factor is 0.27.

bridge position are similar but not identical. Surface A is different from a stoichiometric $RuO_2(110)$ surface. Surface B is identical to a surface where CO resides in the asymmetric bridge position above 2f-cus Ru atoms and occupies all the available 1f-cus Ru atoms in the on-top position. Surface B is similar to surface C (annealed to 210 K) as indicated by an *r* factor of 0.13. The agreement with the structure model in which all 2f-cus Ru and 1f-cus Ru atoms are occupied by CO is, however, worse. This might point toward a loss of on-top CO at 1f-cus Ru atoms, when removing the CO molecules from the low desorption state at 180 K. Flashing the surface to 285 K removes all the on-top CO above the 1f-cus Ru atoms, leaving a surface with CO molecules sitting in asymmetric bridge positions above the 2f-cus Ru atoms. Flashing the surface to 360 K results in a surface structure that is again dominated by the presence of CO in asymmetric bridge positions. Surfaces D and E may differ in terms of the coverage of asymmetric and symmetric bridge CO molecules. The *r* factor between data sets D and E is 0.15, suggesting somewhat different surface structures. On the other hand, the agreement between data sets E and A is 0.05, clearly showing that these surface structures are essentially identical. Finally an anneal to 665 K for 5 minutes leads to a surface structure which is similar to a stoichiometric $RuO_2(110)$ surface. This surface structure is also supported by activity measurements.[22] It was evidenced that a completely reduced $RuO_2(110)$ surface is inactive in oxidizing CO. However, annealing at a temperature above 500 K is able to reactivate such a surface, an effect that was attributed to reappearing bridging O atoms on the surface.

In the following we shall describe in some detail the surface structures of the various CO overlayers on the reduced $RuO_2(110)$ surface which were determined by quantitative LEED in combination with DFT calculations. The preference for particular adsorption sites of CO have already been predicted by the DFT calculations. Exposing a $RuO_2(110)$ surface to 10 L CO at 300 K leads to a surface where all bridging oxygen atoms are replaced by CO molecules in asymmetric bridge positions. We tested various structure models for this experimental LEED data set. The optimum *r*-factor values are collected in Table IV. On the basis of this extended LEED analysis all but two models, where CO molecules bridge the 2f-cus Ru atoms, can clearly be ruled out. Whether the CO molecules are sitting in a symmetric or in an asymmetric bridge position cannot be discriminated from the present LEED analysis. However, DFT calculations resolved this issue by giving a clear preference to the asymmetric bridge position when all 2f-cus Ru atoms are occupied. The structural characteristics of this CO overlayer are depicted in Fig. 4. The agreement between experimental and theoretical LEED data can be judged from Fig. 5. The overall agreement between the structural parameters determined by DFT calculations and quantitative LEED is good. The only parameter value where both techniques significantly differ is the vertical position of the threefold coordinated surface oxygen with respect to the 2f-cus Ru atoms.

Exposing this surface to 5 L CO at 50 K results in a surface structure where both the 2f-cus Ru atoms and the 1f-cus Ru atoms are completely occupied by CO molecules.

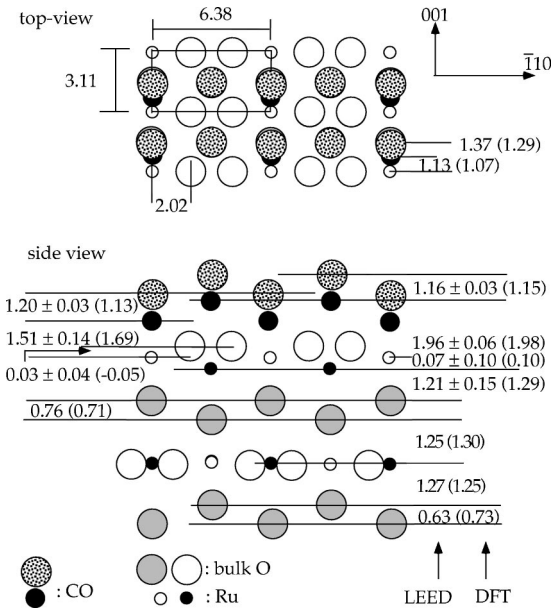

FIG. 6. The optimum surface geometry of the CO on the reduced $RuO_2(110)$ surface, when the stoichiometric $RuO_2(110)$ surface is exposed to 10 L CO at room temperature and then to 5 L CO at 50 K. The structure was determined by LEED and DFT calculations (parameter values are in parentheses). CO sits in an asymmetric bridge position above 2f-cus Ru atoms and occupies all 1f-cus Ru atoms in the on-top position. All values are in angstrom.

CO molecules reside in an asymmetric bridge position above the 2f-cus Ru atoms, and the CO molecules adsorb in on-top positions at the 1f-cus Ru. The surface structure is indicated in Fig. 6, while in Fig. 7 the corresponding calculated LEED

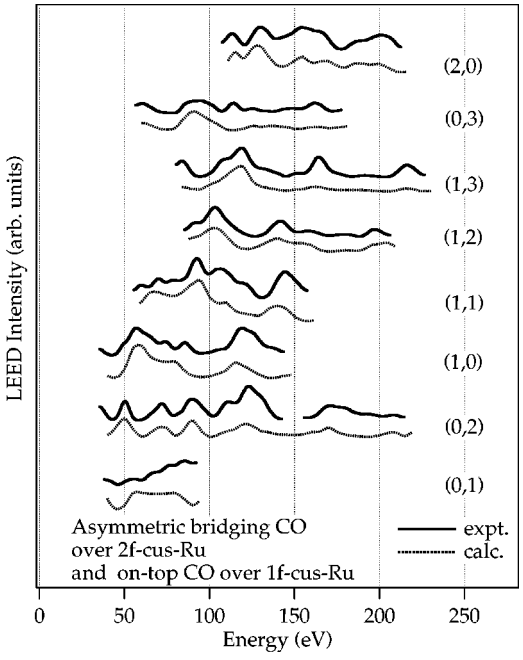

FIG. 7. Comparison of experimental LEED $I(V)$ data and simulated LEED $I(V)$ curves for the CO-$RuO_2(110)$ with CO sitting in both the asymmetric bridge position above 2f-cus Ru atoms and the on-top position above 1f-cus Ru atoms. The optimum R_P factor is 0.29.

data are compared with experimental ones. The latter adsorption site of CO was also determined in a recent LEED/DFT analysis of the CO adsorption on the stoichiometric $RuO_2(110)$ surface.[5]

Probably the most important CO surface structure for gaining a deeper insight into the adsorption behavior of the reduced $RuO_2(110)$ surface is the low CO coverage phase, which is related to surface A. For this reason we tested again various reasonable model surface structures, whose optimum *r* factors are listed in Table V. From this analysis it is clear that surface A is best described by a structure where the CO molecules are sitting in symmetric bridge positions above the 2f-cus Ru atoms. On the average every second bridge position is occupied by CO. Yet, an ordered (2×1) overlayer phase is not formed, very likely due to the high diffusion barrier of CO along the rows of 2f-cus Ru atoms. This result fits nicely to the DFT calculations we presented in Section III A. Moreover, both DFT and LEED calculations revealed that the 2f-cus Ru atoms attached to the CO molecules are drawn towards the CO molecule by about 0.2 Å. This lateral relaxation of the 2f-cus Ru atoms obviously allows for a much better overlap of CO molecular frontier orbitals with those from the substrate. The excellent agreement among the structural parameters determined by DFT and LEED gives further confidence to the determined surface geometry (cf. Fig. 8). The experimental and calculated LEED data sets are compared in Fig. 9. Without CO adsorption, this lateral relaxation of 2f-cus Ru atoms on the $RuO_2(110)$ surface costs 0.29 eV per Ru atom. However, this energy penalty is more than offset by the energy gain due to a better CO bonding to the surface which amounts to 0.87 eV.

At first glance one could think that the asymmetric bridge position is taken by CO because this configuration would reduce the direct repulsion between adjacent CO molecules. This suggestion is not compelling since the CO-CO repulsion can be estimated as the energy difference between on-top CO molecules at 1f-cus Ru atoms in a (2×1) and a (1×1) unit cell, which amounts only to 0.15 eV (cf. Table I). Rather, the asymmetric bridge position of CO is in general

TABLE V. Optimum Pendry's *r* factor achieved with various model structures for surface A. The best *r* factors are given in bold. CO_{s-br}: CO molecules symmetrically bridging 2f-cus Ru atoms. CP_{a-br}: CO molecules asymmetrically bridging 2f-cus Ru atoms. CO_{ot-1f}: CO molecules adsorb on-top of the 1f-cus Ru atoms.

Model structure	Optimum *r* factor
r-$RuO_2(110)$	
0.5 ML CO_{s-br}	**0.26**
1.0 ML CO_{s-br}	0.37
Bare surface	0.32
1.0 ML CO_{ot-1f}	0.75
1.0 ML CO_{a-br}	0.61
0.5 ML CO_{a-br}	0.67
s-$RuO_2(110)$	
Bare surface	0.35
On-top CO above 1f-cus Ru	0.77

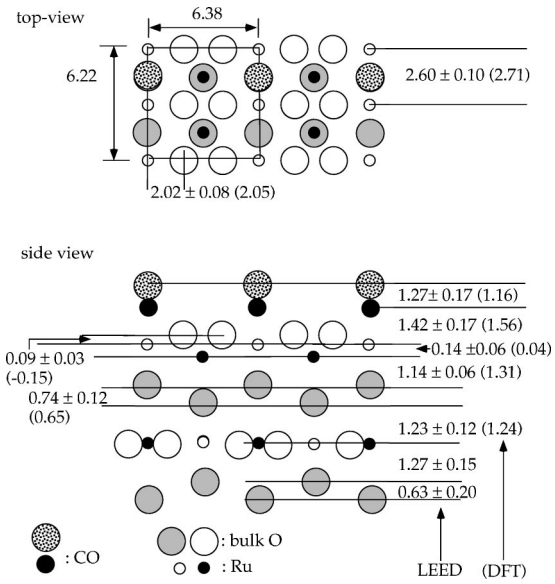

FIG. 8. The optimum surface geometry of surface A, i.e., the stoichiometric $RuO_2(110)$ surface was exposed to 5 L CO at 170 K followed by a short flash to 400 K; this procedure was repeated three times. The resulting structure consists of a reduced $RuO_2(110)$ surface, where (on the average) every second pair of 2f-cus Ru atoms is (symmetrically) bridged by a CO molecule. The atomic geometry was determined by LEED and DFT calculations (parameter values are in parentheses). All values are in angstrom.

the preferred adsorption site when no lateral relaxations of the Ru atoms are considered. This is even true when CO adsorbs into the (2×1) O_{br} vacancy structure. In the (2×1) unit cell, however, the 2f-cus Ru atoms have the freedom to relax towards the CO molecules, thereby optimizing the overlap of CO 5σ and 2π orbitals with appropriate Ru orbitals. When the CO coverage is increased so that every bridge position among the 2f-cus Ru atoms is occupied, a

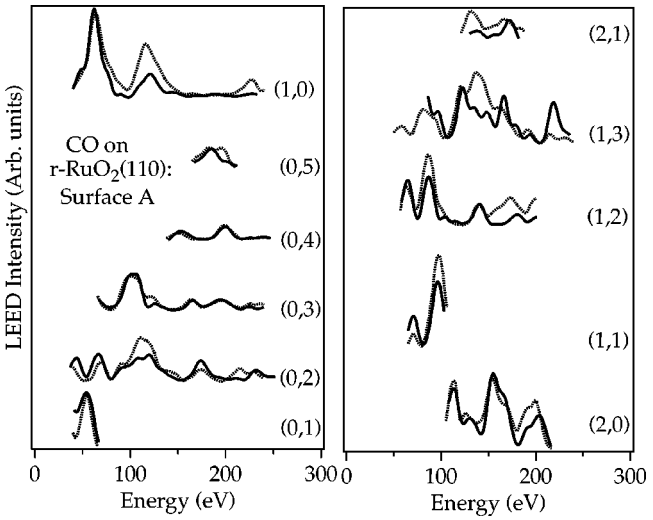

FIG. 9. Comparison of experimental LEED $I(V)$ data and simulated LEED $I(V)$ curves for Surface A, i.e., a reduced $RuO_2(110)$ surface with every second pair of 2f-cus Ru atoms bridged by a CO molecule. The optimum R_P factor is 0.26.

TABLE VI. Comparison of structural and electronic characteristics from DFT calculations among the CO-RuO_2(110) surfaces (either reduced or stoichiometric) and CO-Ru(0001), in particular the internal C-O [d(C-O)] and Ru-C [d(Ru-C)] bond lengths in angstrom. The occupation factors $f_{2\pi}$ of the CO-2π orbital are deduced from the projection of the Kohn-Sham states of the adsorption system on the 2π molecular orbitals. The overlap of noninteracting systems has been subtracted. BE is the CO binding energy in electro volts. CO_{s-br}: CO molecules symmetrically bridging 2f-cus Ru atoms. CO_{a-br}: CO molecules asymmetrically bridging 2f-cus Ru atoms. CO_{ot-1f}: CO molecules adsorb on-top of the 1f-cus Ru atoms. CO_{ot-2f}: CO molecules adsorb on-top of the 2f-cus Ru atoms.

System	d(C-O)	d(Ru-C)	BE	$f_{2\pi}$
Ru(0001)-($\sqrt{3}\times\sqrt{3}$)$R30°$-CO_{ot}	1.16	1.93	1.80	0.40
s-RuO_2(110)-(1×1)-CO_{ot-1f}	1.13	1.95	1.20	0.22
r-RuO_2(110)-(2×1)-CO_{s-br}	1.16	2.06	1.85	0.40
r-RuO_2(110)-(1×1)-CO_{a-br}	1.13	1.99	1.59	0.34
r-RuO_2(110)-(2×1)-CO_{ot-1f}	1.15	1.93	1.61	0.30
r-RuO_2(110)-(1×1)-CO_{ot-1f}	1.14	1.94	1.46	0.29
r-RuO_2(110)-(1×1)-CO_{ot-2f}	1.15	1.94	1.04	0.32

lateral relaxation of the Ru atoms is forbidden on symmetry grounds. The only way to maximize the overlap between the CO orbitals and the Ru orbitals is to modify the local adsorption geometry from the symmetric to asymmetric bridge position. With the observed asymmetric bridge position both the σ donation and π back donation are quite strong.

In Table VI the C-O and the Ru-C bond lengths are compared among the various CO-RuO_2(110) surfaces and the CO-Ru(0001) surface. We collected only values derived from our DFT calculations since the error bars for LEED-derived values are too large to allow for a sensible discussion. The absolute values determined by DFT may also be subject to large error bars but the relative values are reliable since we used in all DFT calculations the same approximations such as the pseudopotentials; systematic errors should therefore be the same, i.e., independent of the particular system under consideration. If the coordination of the CO adsorption is the same, then the Ru-C bond length follows closely the corresponding binding energies: The smaller the binding energy, the longer the Ru-C bond. Table VI reveals also that with increasing coordination number of CO the metal-C bond length increases; this is a quite general phenomenon for CO adsorption on metal surfaces.[23] The internal C-O bond length follows a similar trend: The stronger the CO-surface bond, the longer the internal C-O bond. This trend is even better captured by the population analysis of the CO-2π molecular orbital (last column of Table VI). The more electron density is transferred into the CO-2π orbital, the stronger the CO-surface bonding and the larger the internal C-O bond length; recall that the CO-2π orbital is an antibonding molecular orbital with respect to the internal C-O bonding.

IV. CONCLUSIONS

The adsorption geometries of CO on the stoichiometric and the reduced RuO_2(110) surface were determined by employing the DFT and LEED techniques. On the stoichiometric RuO_2(110) surface, CO molecules adsorb exclusively on top of the onefold undercoordinated Ru atoms (1f-cus Ru).[2] On the reduced RuO_2(110) surface, where the bridging oxygens are stripped off, the CO molecules adsorb first above the twofold undercoordinated Ru atoms (2f-cus Ru) in a symmetric bridge position (binding energy, 1.85 eV) up to a coverage where every second bridge position of 2f-cus Ru atoms are occupied. Beyond this CO coverage, additional CO molecules are accommodated above the 2f-cus Ru atoms, changing the adsorption site from the symmetric to the asymmetric bridge position (averaged binding energy, 1.59 eV). When all 2f-cus Ru atoms have been capped by asymmetric bridging CO molecules, also the 1f-cus Ru atoms become progressively occupied by on-top CO (averaged binding energy, 1.31 eV).

ACKNOWLEDGMENTS

We thank the Leibniz-Rechenzentrum, Munich, for generously providing us computing time.

*Email address: Ari.P.Seitsonen@iki.fi; WWW homepage: http://www.iki.fi/ãpsi/

†Email address: H.Over@FKF.MPG.DE; WWW homepage: http://www.FHI-Berlin.MPG.DE/pc/ Present and permanent address: MPI für Festkörperforschung, Heisenbergstr. 1, D-70569 Stuttgart, Germany.

[1] H. Over, Y.D. Kim, A.P. Seitsonen, S. Wendt, E. Lundgren, M. Schmid, P. Varga, A. Morgante, and G. Ertl, Science **287**, 1474 (2000).

[2] Y.D. Kim, H. Over, G. Krabbes, and G. Ertl, Top. Catal. **14**, 95 (2001).

[3] A. Böttcher, M. Rogazia, H. Niehus, H. Over, and G. Ertl, J. Phys. Chem. **103**, 6267 (1999).

[4] L. Zang and H. Kisch, Angew. Chem. Int. Ed. Engl. **39**, 3921

(2000).
[5] Y.D. Kim, A.P. Seitsonen, and H. Over, Surf. Sci. **465**, 1 (2000).
[6] Y.D. Kim, A.P. Seitsonen, and H. Over, Phys. Rev. B **63**, 115419 (2001).
[7] C.Y. Fan, J. Wang, K. Jacobi, and G. Ertl, J. Chem. Phys. **114**, 10 058 (2001).
[8] H. Over, H. Bludau, M. Skottke-Klein, W. Moritz, and G. Ertl, Phys. Rev. B **46**, 4360 (1992).
[9] W. Moritz, J. Phys. C **17**, 353 (1983).
[10] G. Kleinle, W. Moritz, and G. Ertl, Surf. Sci. **226**, 119 (1990); H. Over, U. Ketterl, W. Moritz, and G. Ertl, Phys. Rev. B **46**, 15 438 (1992); M. Gierer, H. Over, and W. Moritz (unpublished).
[11] J.B. Pendry, J. Phys. C **13**, 93 (1980).
[12] J.P. Perdew, K. Burke, and M. Ernzerhof, Phys. Rev. Lett. **77**, 3865 (1996).
[13] N. Troullier and J.L. Martins, Phys. Rev. B **43**, 1993 (1991).
[14] S.L. Cunningham, Phys. Rev. B **10**, 4988 (1974); A. P. Seitsonen, Ph.D. thesis, Technische Universität Berlin, 2001.
[15] K. Christmann, *Introduction to Surface Physical Chemistry* (Steinkopff, Dresden, 1991).
[16] P.A. Readhead, Vacuum **12**, 203 (1962).
[17] J.H. de Boer, Adv. Catal. **8**, 89 (1956).
[18] H. Pfnür, P. Feulner, and D. Menzel, J. Chem. Phys. **79**, 4613 (1983).
[19] J. Wang, C.F. Fan, K. Jacobi, and G. Ertl, Surf. Sci. **481**, 113 (2001).
[20] See, for instance, M.C. Asensio, D.P. Woodruff, A.W. Robinson, K.-M. Schindler, P. Gardener, D. Ricken, A.M. Bradshaw, and J.C. Conesa, Chem. Phys. Lett. **192**, 259 (1992).
[21] H. Over, M. Gierer, H. Bludau, G. Ertl, and S.Y. Tong, Surf. Sci. **314**, 243 (1994).
[22] S. Wendt, Y. D. Kim, M. Knapp, H. Idriss, and H. Over (unpublished).
[23] H. Over, Prog. Surf. Sci. **58**, 249 (1998).